

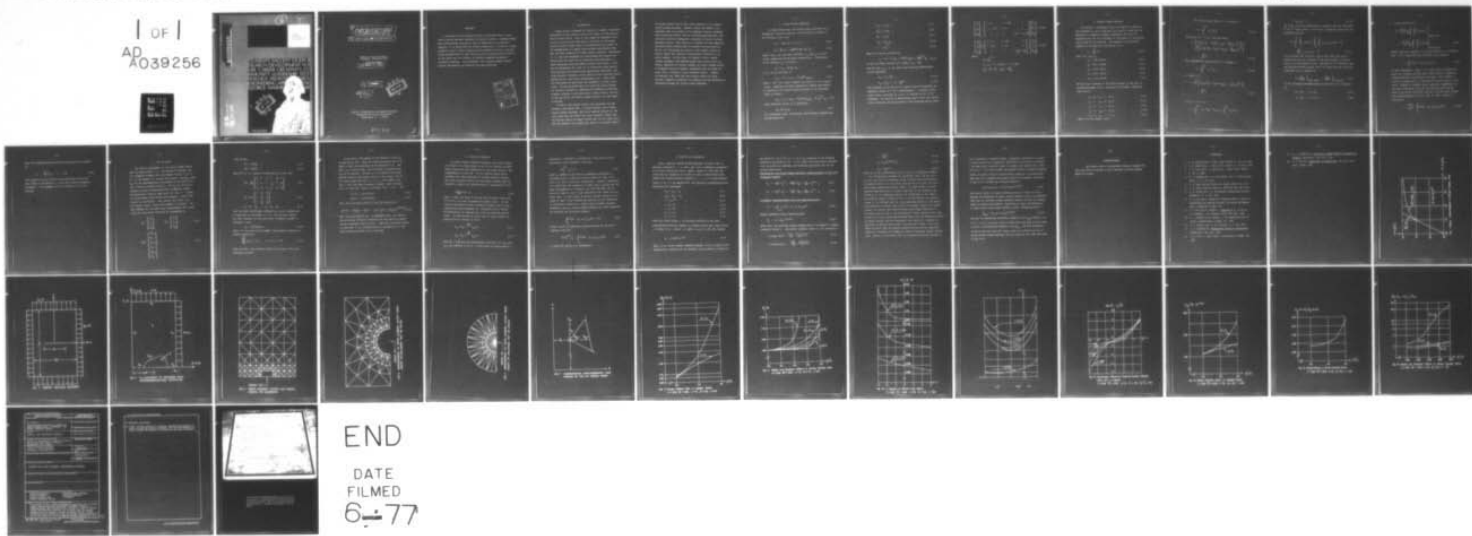
AD-A039 256 GEORGE WASHINGTON UNIV WASHINGTON D C SCHOOL OF ENGI--ETC F/G 20/11
THE NONLINEAR AND BIAXIAL EFFECTS ON ENERGY RELEASE RATE, J-INT--ETC(U)
MAR 77 J D LEE, H LIEBOWITZ N00014-75-C-0946

UNCLASSIFIED

NL

1 OF 1
AD
A039256

ETC
100



END

DATE
FILMED
6-77

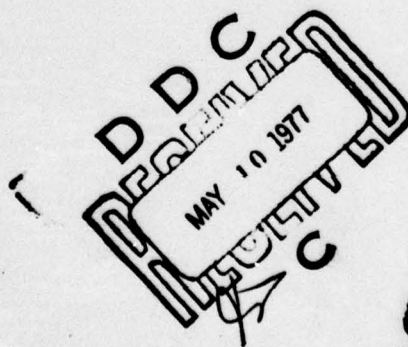


68

ADA U39256

THE
GEORGE
WASHINGTON
UNIVERSITY

STUDENTS FACULTY STUDY R
ESEARCH DEVELOPMENT FUT
URE CAREER CREATIVITY CO
MMUNITY LEADERSHIP TECH
NOLOGY FRONTIERS DESIGN
ENGINEERING APPROPRIENCE
GEORGE WASHINGTON UNIVERSITY



SCHOOL OF ENGINEERING
AND APPLIED SCIENCE

6
THE NONLINEAR AND BIAXIAL EFFECTS
ON ENERGY RELEASE RATE, J-INTEGRAL,
AND STRESS INTENSITY FACTOR

10 James D. Lee ■ Harold Liebowitz

Office of Naval Research
Arlington, Virginia 22217

Contract Number

15 N00014-75-C-0946

11 Mar [redacted] 77



13 42 p.

School of Engineering and Applied Science
The George Washington University
Washington, D. C. 20052

153 370

mt

ABSTRACT

A nonlinear finite element analysis is performed for a finite center-cracked specimen subjected to biaxial loading. A Ramberg-Osgood type stress-strain relation is used to characterize the material property. It is found that the energy release rate, J-integral, stress intensity factor, strain intensity factor depend not only on applied stress perpendicular to the crack but also on applied stress parallel to the crack. Biaxial effects on fracture toughness parameters increase as applied stress increases. The coupling between biaxial effects and material nonlinearity has been indicated.

REQUEST FOR	White Section	<input checked="" type="checkbox"/>
WES	Buff Section	<input type="checkbox"/>
CDG		<input type="checkbox"/>
UNANNOUNCED		<input type="checkbox"/>
JUSTIFICATION		
BY		
DISTRIBUTION/AVAILABILITY CODES		
Dist.	Avail.	or Special
R		

1. Introduction

Linear elastic treatment of fracture is usually considered applicable for net section stress up to about 0.8 the uniaxial tensile yield stress. Even in this range the immediate vicinity of a crack tip has some plastic yield due to the singularity of stress field, hence the distribution of stresses in the neighborhood of a sharp crack differs considerably from what has been predicted by linear elastic analysis. Hutchinson [1, 2], Rice and Rosengren [3] investigated the singular behavior near the crack tip for materials characterized by a power hardening relation between stresses and strains. Goldman and Hutchinson [4], Shih [5, 6] solved the fully plastic crack problems and proposed some approximate functional relations between J-integral, stress and/or strain intensity factor, applied stress, load point displacement, etc. Those works just mentioned are based upon the assumption of small scale yield. Hilton and Hutchinson [7] solved the crack problem for infinite specimen by combining the knowledge of dominant singular solution in the near-field, linear elastic solution in the far-field, and finite element analysis for the region in between.

As far as the biaxial effects are concerned, Lee and Liebowitz [8] showed that, in linear analysis for a finite center-cracked specimen, the stress applied parallel to the line crack does not affect the stress intensity factor and the biaxial effect on energy release rate is less than 0.02%. Sih and Liebowitz [9] showed that there is no biaxial effect

on energy release rate in the linear analysis of an infinite center-cracked specimen. However, Kibler and Roberts [10] indicated that an increase in the apparent fracture toughness with increasing biaxial load was observed experimentally, and this fact can not be adequately explained by linear fracture mechanics theory. This leads us to believe the experimentally observed biaxial effects must be coupled with nonlinearity. Hilton [11] calculated the plastic stress and/or strain intensity factor for infinite cracked plates subjected to biaxial loading. In this work, we analyze a finite center cracked specimen, with Ramberg-Osgood type stress-strain relation, subjected to biaxial loading, by finite element method to obtain fracture toughness parameters such as energy release rate, J-integral, stress intensity factor. Indeed, the analysis has shown that the biaxial effects on those fracture toughness parameters are coupled with the nonlinearity introduced through the stress-strain relations.

2. Stress-Strain Relations

In linear elasticity, the stress-strain relations for a homogeneous isotropic material can be written in either of the following forms [12]:

$$\sigma_{ij} = \lambda \epsilon_{kk} \delta_{ij} + 2\mu \epsilon_{ij}, \quad (2.1)$$

$$\epsilon_{ij} = \frac{1}{2\mu} \sigma_{ij} - \frac{\lambda}{2\mu(3\lambda + 2\mu)} \sigma_{kk} \delta_{ij}, \quad (2.2)$$

where λ and μ are the Lame constants, σ_{ij} and ϵ_{ij} are the stress tensor and strain tensor respectively. Introducing stress deviator s_{ij} as follows:

$$s_{ij} \equiv \sigma_{ij} - \frac{1}{3} \sigma_{kk} \delta_{ij}, \quad (2.3)$$

(2.2) can be rewritten as:

$$E\epsilon_{ij} = (1 + v) s_{ij} + \frac{1 - 2v}{3} \sigma_{kk} \delta_{ij}, \quad (2.4)$$

where E and v are Young's modulus and Poisson's ratio respectively. Adopting the model suggested by Ramberg and Osgood, we generalize the stress-strain relations to the nonlinear range as follows:

$$E\epsilon_{ij} = (1 + v)s_{ij} + \frac{1 - 2v}{3} \sigma_{kk} \delta_{ij} + \frac{3}{2} \alpha \sigma_e^{n-1} s_{ij}, \quad (2.5)$$

where effective stress σ_e is defined as:

$$\sigma_e^2 \equiv \frac{3}{2} s_{ij} s_{ij}. \quad (2.6)$$

For convenience sake, we introduce the following nondimensionalized quantities:

$$\bar{\sigma}_{ij} \equiv \sigma_{ij}/\sigma_Y , \quad (2.7)$$

$$\bar{s}_{ij} \equiv s_{ij}/\sigma_Y , \quad (2.8)$$

$$\bar{\sigma}_e \equiv \sigma_e/\sigma_Y , \quad (2.9)$$

$$\bar{\epsilon}_{ij} \equiv E\epsilon_{ij}/\sigma_Y , \quad (2.10)$$

$$\bar{\alpha} \equiv \alpha \sigma_Y^{n-1} . \quad (2.11)$$

Then (2.5) can be rewritten as:

$$\bar{\epsilon}_{ij} = (1 + v) \bar{s}_{ij} + \frac{1 - 2v}{3} \bar{\sigma}_{kk} \delta_{ij} + \frac{3}{2} \bar{\alpha} \sigma_e^{n-1} \bar{s}_{ij} \quad (2.12)$$

In case of simple tension test, namely, $\sigma_{11} = \bar{\sigma}\sigma_Y$

and all other $\sigma_{ij} = 0$, we obtain the following nonvanishing strain components:

$$\bar{\epsilon}_{11} = \bar{\sigma} + \bar{\alpha} \bar{\sigma}^n , \quad (2.13)$$

$$\bar{\epsilon}_{22} = \bar{\epsilon}_{33} = -v\bar{\sigma} - \frac{1}{2} \bar{\alpha} \bar{\sigma}^n . \quad (2.14)$$

The equations (2.13) and (2.14) could be used to determine the numerical values of v , $\bar{\alpha}$, n experimentally. A typical stress-strain curve, according to (2.13), is plotted in Fig. 1 for reference. In the case of generalized plane stress, the stress-strain relations can be expressed in the following matrix forms:

$$\begin{vmatrix} \bar{\epsilon}_x \\ \bar{\epsilon}_y \\ 2\bar{\epsilon}_{xy} \end{vmatrix} = \begin{vmatrix} 1 + g & -v - g/2 & 0 \\ -v - g/2 & 1 + g & 0 \\ 0 & 0 & 2(1 + v) + 3g \end{vmatrix} \begin{vmatrix} \bar{\sigma}_x \\ \bar{\sigma}_y \\ \bar{\sigma}_{xy} \end{vmatrix}, \quad (2.15)$$

$$\begin{vmatrix} \bar{\sigma}_x \\ \bar{\sigma}_y \\ \bar{\sigma}_{xy} \end{vmatrix} = \frac{1}{\gamma} \begin{vmatrix} 1 + g & v + g/2 & 0 \\ v + g/2 & 1 + g & 0 \\ 0 & 0 & \frac{1 - v}{2} + \frac{g}{4} \end{vmatrix} \begin{vmatrix} \bar{\epsilon}_x \\ \bar{\epsilon}_y \\ 2\bar{\epsilon}_{xy} \end{vmatrix}, \quad (2.16)$$

where

$$g \equiv \bar{\alpha} \bar{\sigma}_e^{n-1},$$

$$\gamma \equiv (1 + v + 1.5g)(1 - v + 0.5g),$$

$$\bar{\sigma}_e^2 = \bar{\sigma}_x^2 + \bar{\sigma}_y^2 - \bar{\sigma}_x \bar{\sigma}_y + 3\bar{\sigma}_{xy}^2.$$

3. Center-Cracked Specimen

We consider a rectangular plate of length $2L$, width $2W$, and thickness B , with a centered line crack of crack size $2a$ subjected to symmetric boundary conditions (cf. Fig. 2). Therefore only the first quadrant of the plate $R = [x, y | 0 \leq x \leq W, 0 \leq y \leq L]$ needs to be analyzed. The boundary S of the first quadrant is divided into five parts, i.e.,

$$S = \sum_{i=1}^5 S_i , \quad (3.1)$$

where (cf. Fig. 3)

$$S_1 = [x=W, 0 \leq y \leq L] , \quad (3.2)$$

$$S_2 = [y=L, 0 \leq x \leq W] , \quad (3.3)$$

$$S_3 = [x=0, 0 \leq y \leq L] , \quad (3.4)$$

$$S_4 = [y=0, 0 \leq x \leq a] , \quad (3.5)$$

$$S_5 = [y=0, a \leq x \leq W] . \quad (3.6)$$

We focus our attention on the plane problem, in the case of generalized plane stress, which has the boundary conditions specified by:

$$\sigma_x = k\sigma, \sigma_{xy} = 0 \text{ on } S_1 , \quad (3.7)$$

$$\sigma_y = \sigma, \sigma_{xy} = 0 \text{ on } S_2 , \quad (3.8)$$

$$u_x = 0, \sigma_{xy} = 0 \text{ on } S_3 , \quad (3.9)$$

$$\sigma_y = 0, \sigma_{xy} = 0 \text{ on } S_4 , \quad (3.10)$$

$$u_y = 0, \sigma_{xy} = 0 \text{ on } S_5 . \quad (3.11)$$

where k is the biaxial factor.

The strain energy density U is defined as:

$$U \equiv \int_0^{\epsilon_{ij}} \sigma_{ij} d\epsilon_{ij} \quad (3.12)$$

Utilizing (2.5 - 2.11), one may obtain

$$\begin{aligned} U &= \left\{ \frac{1+v}{3} \sigma_e^2 + \frac{1-2v}{6} (\sigma_{kk})^2 + \frac{\alpha n}{n+1} \sigma_e^{n+1} \right\} / E \\ &= \frac{\sigma_Y^2}{E} \left\{ \frac{1+v}{3} \bar{\sigma}_e^2 + \frac{1-2v}{6} (\bar{\sigma}_{kk})^2 + \frac{\bar{\alpha} n}{n+1} \bar{\sigma}_e^{n+1} \right\} \\ &\equiv \frac{\sigma_Y^2}{E} U \end{aligned} \quad (3.13)$$

The complementary energy density V , defined as

$$V \equiv \int_0^{\sigma_{ij}} \epsilon_{ij} d\sigma_{ij} \quad (3.14)$$

is found to be

$$\begin{aligned} V &= \frac{\sigma_Y^2}{E} \left\{ \frac{1+v}{3} \bar{\sigma}_e^2 + \frac{1-2v}{6} (\bar{\sigma}_{kk})^2 + \frac{\bar{\alpha} n}{n+1} \bar{\sigma}_e^{n+1} \right\} \\ &\equiv \frac{\sigma_Y^2}{E} V \end{aligned} \quad (3.15)$$

related to each other as

$$V = \int_0^{\sigma_{ij}} \epsilon_{ij} d\sigma_{ij} = \epsilon_{ij} \sigma_{ij} - \int_0^{\epsilon_{ij}} \sigma_{ij} d\sigma_{ij}$$

$$= \sigma_{ij} \epsilon_{ij} - U , \quad (3.16)$$

the total strain and complementary energies, per unit thickness, U^* and V^* respectively, of the whole rectangular plate have the following relation

$$\begin{aligned} V^* &\equiv \int_{-W}^W \int_{-L}^L V \, dx \, dy = \int_{-W}^W \int_{-L}^L \sigma_{ij} u_{i,j} \, dx \, dy - U^* \\ &= \oint \sigma_{ij} n_j u_i \, ds - U^* . \end{aligned} \quad (3.17)$$

It is noticed that the first term on the right hand side is nothing but the line integral of the inner product of stress vector and displacement vector. Equation (3.17) indicates that the nonlinear energy release rate \tilde{G} in fixed load and fixed grip situations can be obtained as

$$\tilde{G} = \frac{\partial V^*}{\partial(2a)} \Big|_{\text{fixed load}} = - \frac{\partial U^*}{\partial(2a)} \Big|_{\text{fixed grip}} \quad (3.18)$$

If the following nondimensionalized quantities are introduced as

$$\bar{x} \equiv x/W , \quad \bar{y} \equiv y/W , \quad (3.19)$$

$$\ell \equiv L/W , \quad c \equiv a/W , \quad (3.20)$$

\tilde{G} can be rewritten as:

$$\begin{aligned}\tilde{G} &= \frac{2W \sigma_Y^2}{E} \frac{\partial}{\partial c} \int_0^1 \int_0^l \bar{V} d\bar{x} d\bar{y} && \text{fixed load} \\ &= - \frac{2W \sigma_Y^2}{E} \frac{\partial}{\partial c} \int_0^1 \int_0^l \bar{U} d\bar{x} d\bar{y} && \text{fixed grip}\end{aligned}\quad (3.21)$$

Another important quantity in fracture mechanics is J-integral [13]. It is stated that the following line integral J

$$J \equiv \int_{\Gamma} (U dy - \sigma_{ij} n_j u_{i,x} ds) \quad (3.22)$$

is path-independent. Here, Γ is a curve which surrounds the crack tip, starting from the lower crack surface, traversing counterclockwise, and ending on the upper crack surface, s is the arc length and n_i is outward unit vector normal to the curve. Because of symmetry and J being path independent, we can pick up any point on S_5 as the starting point and any point on S_4 as the end point, and let Γ_{12} be any curve traversing counterclockwise in R (cf. Fig. 3), then J can be re-written as:

$$J = \frac{2W \sigma_Y^2}{E} \int_{\Gamma_{12}} (\bar{U} d\bar{y} - \bar{\sigma}_{ij} n_j \bar{u}_{i,\bar{x}} d\bar{s}), \quad (3.23)$$

where the nondimensionalized quantities \bar{u}_i and \bar{s} are defined as:

$$u_i \equiv \frac{\sigma_Y W}{E} \bar{u}_i , \quad \bar{s} \equiv s/W . \quad (3.24)$$

This problem will be solved by using nonlinear finite-element method to determine \tilde{G} , J , and other fracture toughness parameters. The procedure will be discussed in the next section.

4. The Procedure

The typical arrangement of the finite element layout with 212 nodal points, i.e., 424 degrees of freedom, and 377 triangular elements are illustrated in Figs. 4, 5, 6. If j is the number of a certain nodal point, then \bar{u}_{2j-1} and \bar{u}_{2j} are the nondimensional displacement of the point in x and y direction respectively, \bar{F}_{2j-1} and \bar{F}_{2j} are the corresponding external concentrated force components (nondimensionalized) acting on that point (cf. Fig. 7). Assume the displacement field within each element is linear with respect to coordinates. This implies the strain, and accordingly stress, within each element is constant. For each element let the nodal point displacements $[\bar{\delta}]$, strain field $[\bar{\epsilon}]$, and stress field $[\bar{\sigma}]$ be represented by

$$[\bar{\epsilon}] \equiv \begin{vmatrix} \bar{\epsilon}_x \\ \bar{\epsilon}_y \\ 2\bar{\epsilon}_{xy} \end{vmatrix}, \quad [\bar{\sigma}] \equiv \begin{vmatrix} \bar{\sigma}_x \\ \bar{\sigma}_y \\ \bar{\sigma}_{xy} \end{vmatrix}, \quad (4.1)$$

$$[\bar{\delta}] \equiv \begin{vmatrix} \bar{u}_{2i-1} \\ \bar{u}_{2i} \\ \bar{u}_{2j-1} \\ \bar{u}_{2j} \\ \bar{u}_{2k-1} \\ \bar{u}_{2k} \end{vmatrix}, \quad (4.2)$$

then we have

$$[\bar{\epsilon}] = [B][\bar{\delta}] , \quad (4.3)$$

$$[\bar{\sigma}] = [D][\bar{\epsilon}] , \quad (4.4)$$

where $[D]$ is 3×3 matrix as indicated in (2.16), and

$$[B] = \frac{1}{2\Delta} \begin{vmatrix} b_i & 0 & b_j & 0 & b_k & 0 \\ 0 & c_i & 0 & c_j & 0 & c_k \\ c_i & b_i & c_j & b_j & c_k & b_k \end{vmatrix} , \quad (4.5)$$

$$2\Delta = \det \begin{vmatrix} 1 & \bar{x}_i & \bar{y}_i \\ 1 & \bar{x}_j & \bar{y}_j \\ 1 & \bar{x}_k & \bar{y}_k \end{vmatrix} , \quad (4.6)$$

$$b_i = \bar{y}_j - \bar{y}_k , \quad c_i = \bar{x}_j - \bar{x}_k , \quad (4.7)$$

with the other coefficients obtained by a cyclic permutation of subscripts in the order i, j, k . The stiffness matrix per unit thickness of this particular triangular element is obtained as [14]:

$$[k] = [B]^T [D] [B] A , \quad (4.8)$$

where A is the area of the element. The governing equation is finally obtained as:

424

$$\sum_{\gamma=1}^{424} K_{\beta\gamma} \bar{u}_{\gamma} = \bar{F}_{\beta} , \quad \beta = 1, 2, \dots, 424 \quad (4.9)$$

where the 424×424 stiffness matrix is the sum of 377 local stiffness matrices.

Since matrix $[D]$ depends on the effective stress $\bar{\sigma}_e$, so does matrix $[K]$. Thus, an iteration process has to be taken to solve the nonlinear matrix equation (4.9). And also, it is noticed that the principle of superposition can not be applied. Therefore, for a specifically given applied stress σ and biaxial factor k , we assign a set of 377 trial values for $g(I)$, $I = 1, 2, \dots, 377$, namely, let $g(I) = g^*(I)$ for each triangular element. After solving (4.9), we have \bar{u}_Y^* , then we calculate, for $I = 1, 2, \dots, 377$,

$$[\bar{\epsilon}(I)] = [B(I)][\bar{\delta}(I)] , \quad (4.10)$$

$$[\bar{\sigma}(I)] = [D(I)][\bar{\epsilon}(I)] . \quad (4.11)$$

Thus, the calculated values of $g(I)$ are obtained as:

$$g^{**}(I) = \bar{\alpha}[\bar{\sigma}_x^2(I) + \bar{\sigma}_y^2(I) - \bar{\sigma}_x(I)\bar{\sigma}_y(I) + 3\bar{\sigma}_{xy}^2(I)]^{(n-1)/2} \quad (4.12)$$

This iteration process will be continued until, for each I , the percentage difference between $g^*(I)$ and $g^{**}(I)$ is below certain allowable value of error. After the iteration process is completed, it is straightforward to calculate \tilde{G} , J , and other quantities which we are concerned.

5. Crack Tip Solution

In linear elastic fracture mechanics, the stress intensity factor K is often taken as one of the fracture criteria since K describes the singularity of the stress field in the neighborhood of crack tip. For an infinite plate with a centered line crack subjected to uniform uniaxial tension, the stress intensity factor and the energy release rate are related by Irwin's K-G relation which is represented as [9]:

$$\frac{K^2 \pi (\kappa + 1)}{8\mu} = G , \quad (5.1)$$

where κ takes the value $(3-4v)$ for case of plane strain and $(3-v)/(1+v)$ for case of generalized plane stress. In the case of nonlinearity being introduced through stress-strain relation Rice and Rosengren [3], Hutchinson [1,2], Hilton and Hutchinson [7] obtained the crack tip solution analytically. In this section we recall some of those results in plane stress as follows (cf.[1]):

$$\bar{\sigma}_{ij} = K_\sigma \bar{r}^{-\frac{1}{n+1}} \tilde{\sigma}_{ij}(\theta) , \quad (5.2)$$

$$\bar{\epsilon}_{ij} = K_\epsilon \bar{r}^{-\frac{n}{n+1}} \tilde{\epsilon}_{ij}(\theta) , \quad (5.3)$$

where $K_\epsilon = \bar{\alpha} \bar{K}_\sigma^n$ and the dimensionless functions of θ , $\tilde{\sigma}_{ij}$ and $\tilde{\epsilon}_{ij}$, are detailed in [1,2]. In the crack tip region the di-

dimensionless J-integral is obtained as a function of the dimensionless stress intensity factor \bar{K}_σ :

$$\bar{\alpha} \bar{K}_\sigma^{n+1} c_n = J, \quad (5.4)$$

where c_n depends on the material hardening coefficient n .

In plane stress c_n takes the typical values of 3.86, 3.41, 3.03, 2.87 for $n = 3, 5, 9, 13$ respectively. However, Hutchinson [1], based upon the assumption of small scale yielding and the path independence of J-integral, set the left-hand side of eqn. (5.4) equal to the J value obtained in the linear and uniaxial case. In this study, we do not restrict ourself in the range of small scale yielding and moreover we are interested in the biaxial effects on a finite center-cracked specimen. Therefore, once the finite-element analysis has been completed, we calculate the following integral,

$$\int_{\Gamma_2} (\bar{U} d\bar{y} - \bar{\sigma}_{ij} n_j \bar{u}_{i,\bar{x}} d\bar{s}) \equiv J/2, \quad (5.5)$$

along a curve Γ_2 traversing counterclockwise in the first quadrant R and set

$$2\bar{\alpha} \bar{K}_\sigma^{n+1} c_n = \int_{\Gamma_2} (\bar{U} d\bar{y} - \bar{\sigma}_{ij} n_k \bar{u}_{i,\bar{x}} d\bar{s}) \quad (5.6)$$

to obtain \bar{K}_σ and \bar{K}_ϵ as a consequence.

6. Results and Discussion

Given a specific center-cracked specimen, we have a set of material constants E , ν , α , and n and a set of geometric parameters of a finite rectangular plate, namely, length $2L$, width $2W$, and crack size $2a$. Attention is focused on case of generalized plane stress with uniform biaxial stresses $\sigma_y = \sigma$, $\sigma_x = k\sigma$ being applied along $y = \pm L$, $x = \pm W$ respectively. The following nondimensionalized quantities are introduced:

$$\bar{\sigma}_{ij} = \sigma_{ij} / \sigma_y , \quad (6.1)$$

$$\bar{\epsilon}_{ij} = E\epsilon_{ij} / \sigma_y , \quad (6.2)$$

$$\bar{\alpha} = \alpha \sigma_y^{n-1} , \quad (6.3)$$

$$c = a / W , \quad (6.4)$$

$$l = L / W , \quad (6.5)$$

$$\bar{x} = x / W , \quad (6.6)$$

$$\bar{y} = y / W , \quad (6.7)$$

where the yield stress σ_y is obtained according to the usual engineering definition, namely, in simple tension test, when stress σ is equal to σ_y , strain ϵ is equal to $\sigma_y/E + 0.002$ (cf. Sechler

$$\sigma_y = (0.002 E/\alpha)^{1/n} \quad (6.8)$$

Then, in the finite-element computer program, (2.16) is used as the stress-strain relation and the boundary value problem is solved for

the region $\bar{R} = [\bar{x}, \bar{y} | 0 \leq \bar{x} \leq 1, 0 \leq \bar{y} \leq l]$ according to the boundary conditions specified by (3.7 - 3.11). After the grand matrix equation (4.9) is solved by iteration, the following quantities will be calculated numerically:

Complementary and strain energy densities (dimensionless) in the I-th triangular element :

$$\bar{V}_I = \left\{ \frac{1+v}{3} \bar{\sigma}_e^2 + \frac{1-2v}{6} \bar{\sigma}_{kk}^2 + \frac{\bar{a}}{n+1} \bar{\sigma}_e^{n+1} \right\}_I \quad (6.9)$$

$$\bar{U}_I = \left\{ \frac{1+v}{3} \bar{\sigma}_e^2 + \frac{1-2v}{6} \bar{\sigma}_{kk}^2 + \frac{\bar{a}n}{n+1} \bar{\sigma}_e^{n+1} \right\}_I \quad (6.10)$$

J-integral (dimensionless) along any specified curve Γ :

$$\bar{J} = 2 \int_{\Gamma_{1/2}} (\bar{U} d\bar{y} - \bar{\sigma}_{ij} n_j \bar{u}_{i,\bar{x}} d\bar{s}) \quad (6.11)$$

Stress intensity factor (dimensionless) :

$$\bar{K}_s = (\bar{J} / \bar{a}c_n)^{1/(n+1)} \quad (6.12)$$

After that, the nonlinear energy release rate \bar{G} , J-integral J , stress intensity factor K_s , and strain intensity factor K are obtained as

$$\bar{G} \text{ (fixed load)} = \frac{2W\sigma_Y}{E} \frac{d(\sum A_I V_I)}{dc} \quad , \quad (6.13)$$

$$\bar{G} \text{ (fixed grip)} = - \frac{2W\sigma_Y^2}{E} \frac{d(\sum \bar{A}_I \bar{U}_I)}{dc} \quad , \quad (6.14)$$

$$J = \frac{W\sigma_Y^2}{E} \bar{J} \quad , \quad (6.15)$$

$$K_\sigma = \sigma_Y W^{1/(n+1)} \bar{K}_\sigma \quad , \quad (6.16)$$

$$K_\epsilon = \frac{\alpha}{E} K^n \quad , \quad (6.17)$$

where \bar{A}_I is the dimensionless area of the I-th triangular element.

For illustrative purpose, we fix $\bar{\alpha}=0.02$, $n=13$, $v=0.33$, $\ell=2.5$ in this work and plot nonlinear energy release rate \tilde{G} as function of applied stress σ for two cases, $k=0$ and $k=-3$, at $c=0.5$ in Fig.8 which shows significant biaxial effect. In other words, \tilde{G} in the tension-compression case is higher than that in the uniaxial case. In Fig.9, \tilde{G} , for different values of k , normalized by the linear and uniaxial energy release rate \bar{G} , is plotted against the applied stress. It is noticed that for σ/σ_Y being less than 0.3, the values of \tilde{G} decrease as biaxial load factor k increases, however, at higher stress, one notices that $\tilde{G}(k=3)$ becomes even larger than $\tilde{G}(k=-1)$. We believe this is due to the nonlinearity mainly caused by the large stress $k\sigma$ ($=1.2\sigma_Y$) being applied along $x=+W$. Also the nonlinear effects on energy release rate are remarkable. The values of J-integral as functions of biaxial load factor k are plotted in Figs. 10-11 from which we notice that the general characteristics and the numerical values of J-integral are similar to those of nonlinear energy release rate. However, we do detect that the numerical difference between \tilde{G}

and J increases as applied stress σ increases, especially at larger k values (positive or negative). From Fig.12 we see that G is about 7.8% lower than J when $k=-3$ and it is about 4.4% higher than J when $k=3$ at $\sigma/\sigma_y = 0.4$ and $c=0.505$. The biaxial effect on stress intensity factor is shown in Fig.13 and, relatively speaking, it is much less than that on J -integral and energy release rate because, according to eqn.(5.4), we have the following relation:

$$K_\sigma(k)/K_\sigma(k=0) = [J(k)/J(k=0)]^{1/(n+1)} . \quad (6.18)$$

The biaxial effect on strain intensity factor is shown in Fig.14. Because the dimension of linear stress intensity factor is different than that of nonlinear stress intensity factor, one can not compare these two quantities directly. Therefore we recall the definition of small scale yield stress intensity factor (dimensionless) [1]

$$\bar{K}_{ssy} = [(\sigma/\sigma_y)^2 c_n/\bar{a} c_n]^{1/(n+1)} . \quad (6.19)$$

and plot the percentage difference between K_σ and K_{ssy} against σ/σ_y for $k = -3, 0, 3$ in Fig.15. Also we found that even when $\sigma/\sigma_y \rightarrow 0$, there is still a 2% difference between K_σ and K_{ssy} and this difference is due to the fact that the linear value of J -integral for an infinite center-cracked specimen has been used for the right hand side of eqn.(5.4).

ACKNOWLEDGMENT

The authors wish to acknowledge financial support for this work from the Office of Naval Research, Contract Number N00014-75-C-0946.

REFERENCES

1. J. W. Hutchinson, *J. Mech. Phys. Solids*, V. 16, 13, 1968.
2. J. W. Hutchinson, *J. Mech. Phys. Solids*, V. 16, 337, 1968.
3. J. R. Rice and G. F. Rosengren, *J. Mech. Phys. Solids*, V. 16, 1, 1968.
4. N. L. Goldman and J. W. Hutchinson, *Int. J. Solids Structures*, V. 11, 575, 1975.
5. C. F. Shih, *Harvard University Report DEAP S-10*, 1974.
6. C. F. Shih, *Fracture Analysis*, *ASTM STP 560*, 187, 1974.
7. P. D. Hilton and J. W. Hutchinson, *Engineering Fracture Mechanics*, V. 3, 435, 1971.
8. J. D. Lee and H. Liebowitz, *Technical Report, School of Engineering and Applied Science, The George Washington Univ.*, Submitted to ONR, 1975.
9. G. C. Sih and H. Liebowitz, Fracture V. 2, edited by H. Liebowitz, 67, Academic Press, New York, 1968.
10. J. J. Kibler and R. Roberts, *J. of Engineering for Industry, Transactions of ASME*, 727, 1970.
11. P. D. Hilton, *Int. J. of Fracture*, V. 9, 149, 1973.
12. I. S. Sokolnikoff, Mathematical Theory of Elasticity, McGraw-Hill, New York, 1956.
13. J. R. Rice, *J. Appl. Mech., Transactions of ASME*, 379, 1968.

14. O. C. Zienkiewicz, The Finite Element Method in Engineering Science, McGraw-Hill, New York, 1971.
15. E. E. Sechler, Elasticity in Engineering, John Wiley and Sons, London, 1952.

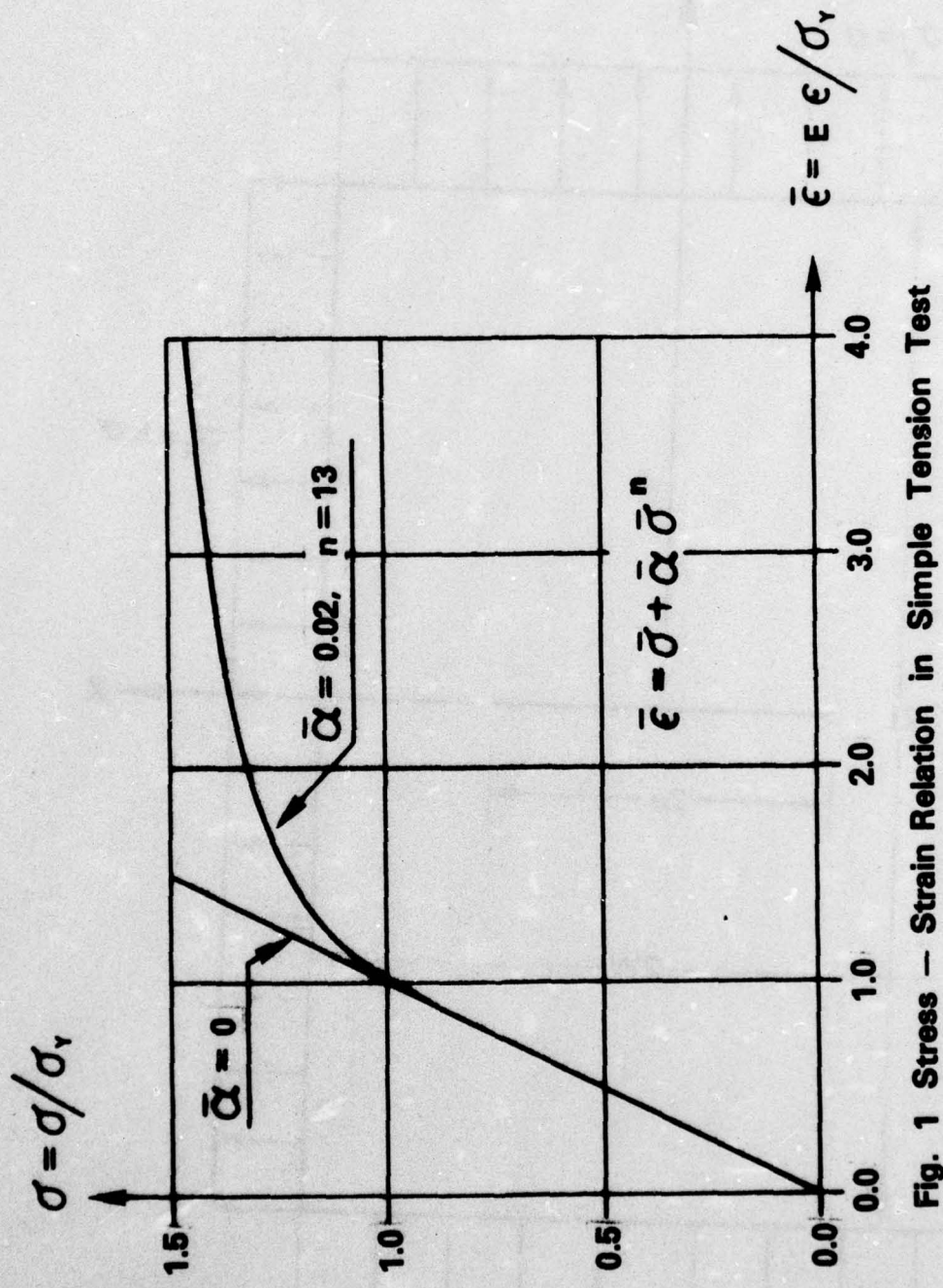


Fig. 1 Stress – Strain Relation in Simple Tension Test

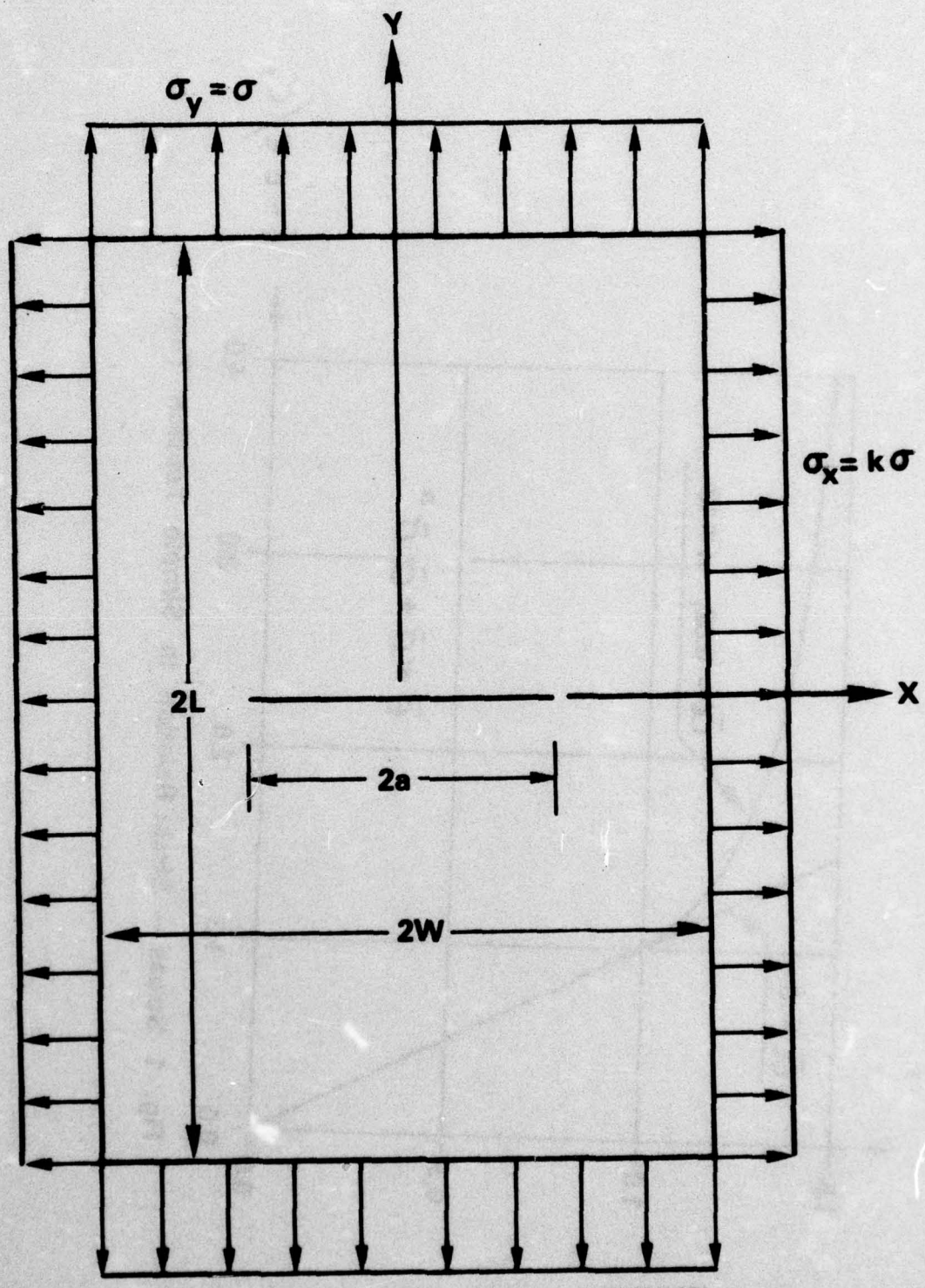


FIG. 2 CENTER - CRACKED SPECIMEN

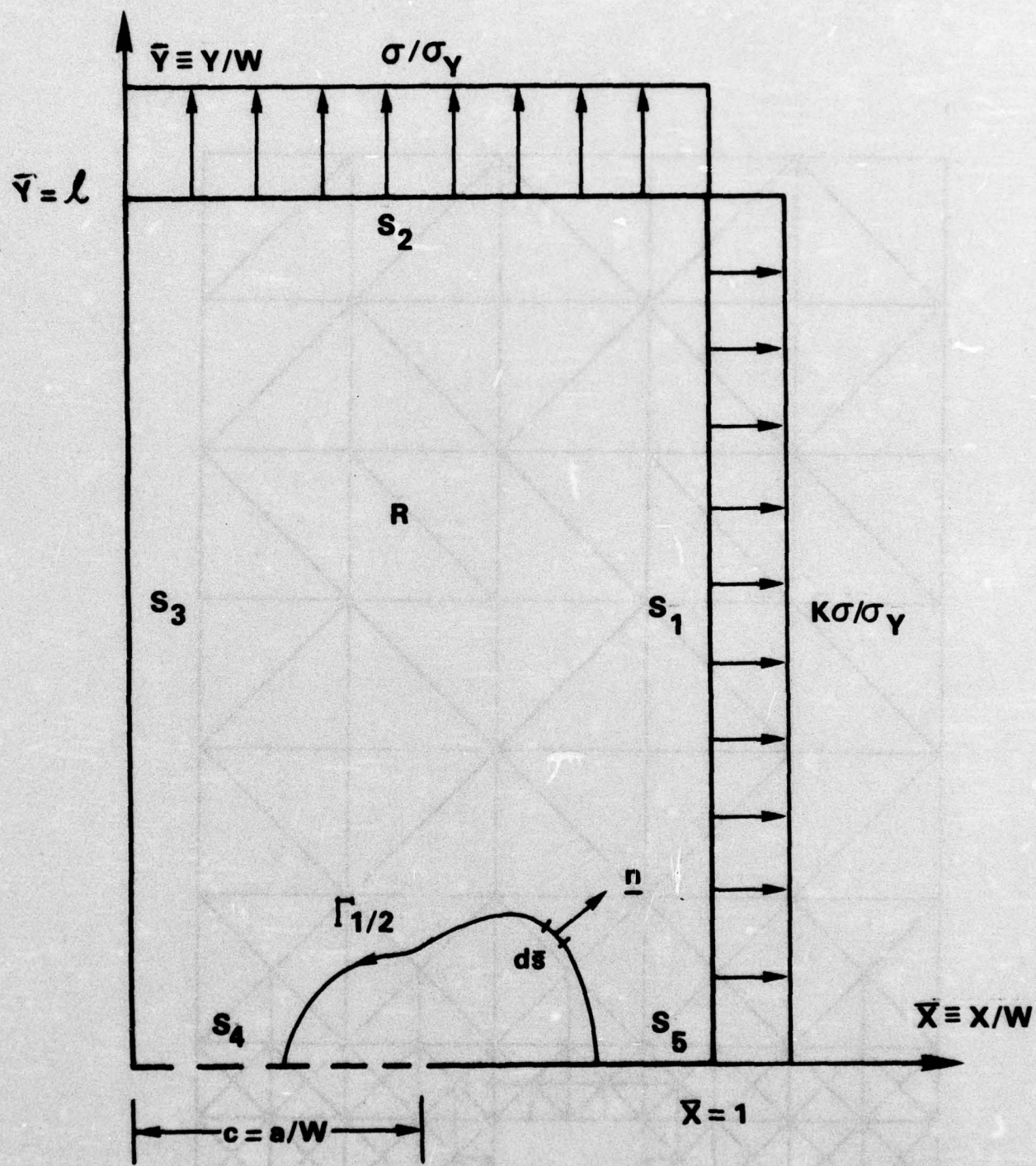


FIG. 3 1st QUADRANT OF SPECIMEN WITH NONDIMENSIONALIZED QUANTITIES

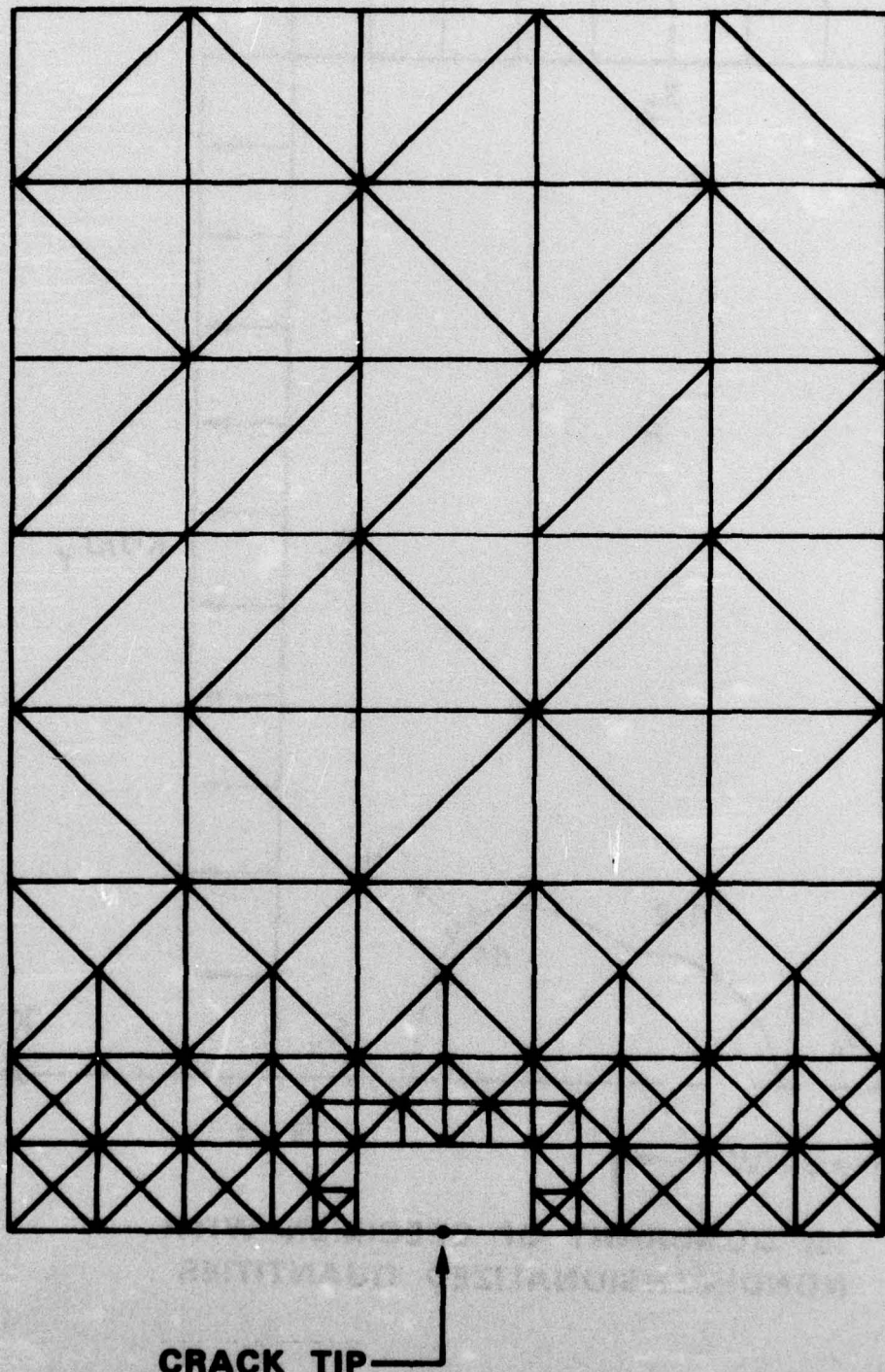


FIG. 4 FINITE ELEMENT LAYOUT (212 NODAL POINTS, 377 ELEMENTS)

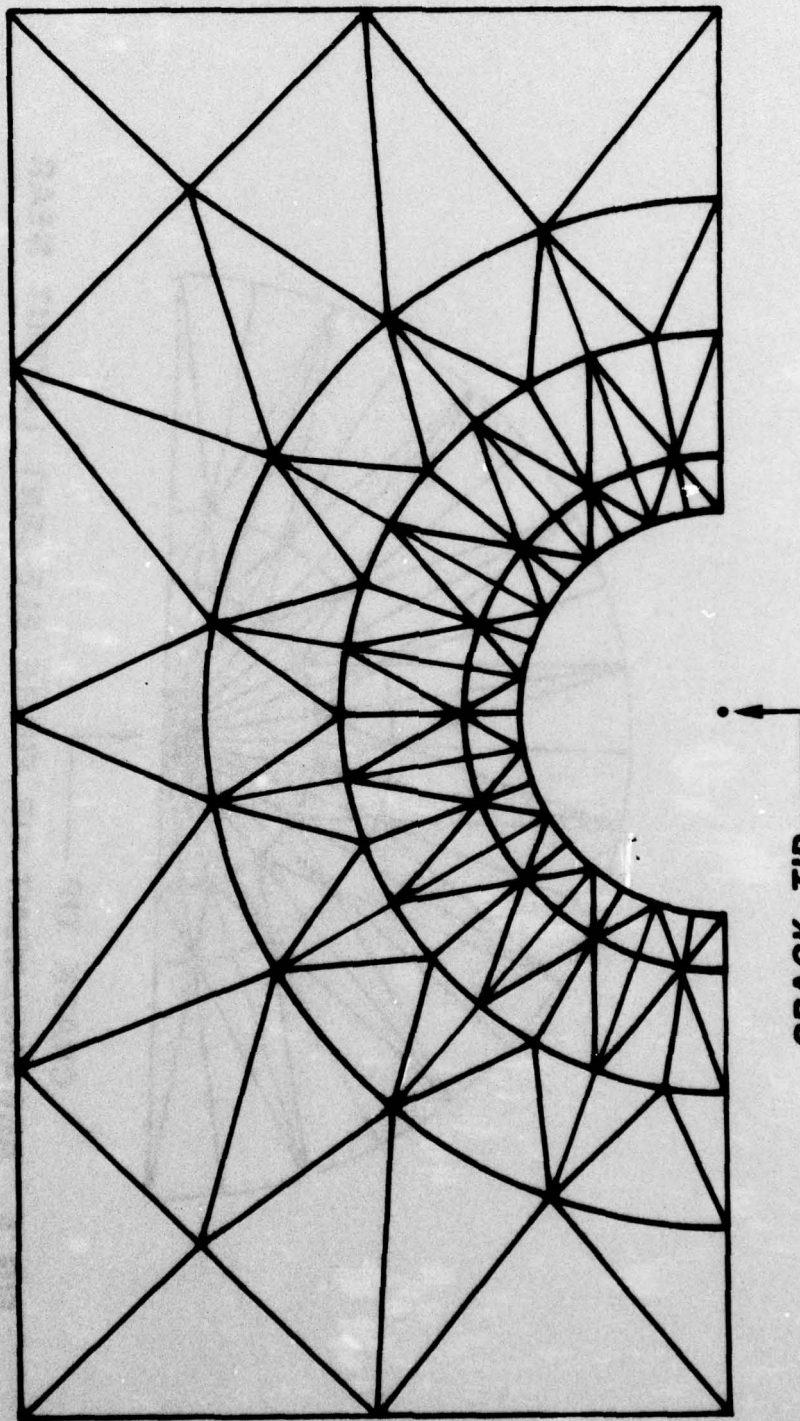


FIG. 5 ARRANGEMENT OF FINITE ELEMENT LAYOUT NEAR
CRACK TIP (ENLARGED, NOT ON SCALE)

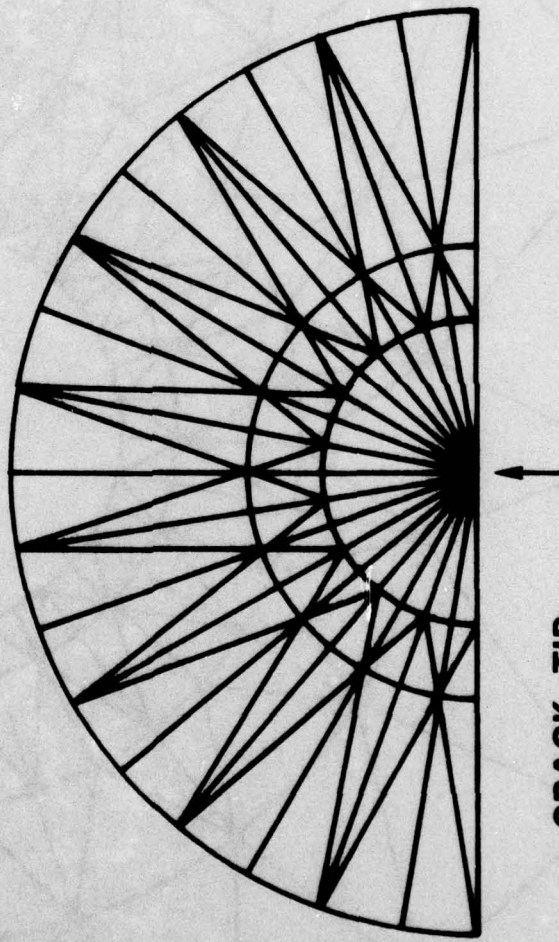


FIG. 6 ARRANGEMENT OF FINITE ELEMENT LAYOUT NEAR
CRACK TIP (ENLARGED, NOT ON SCALE)

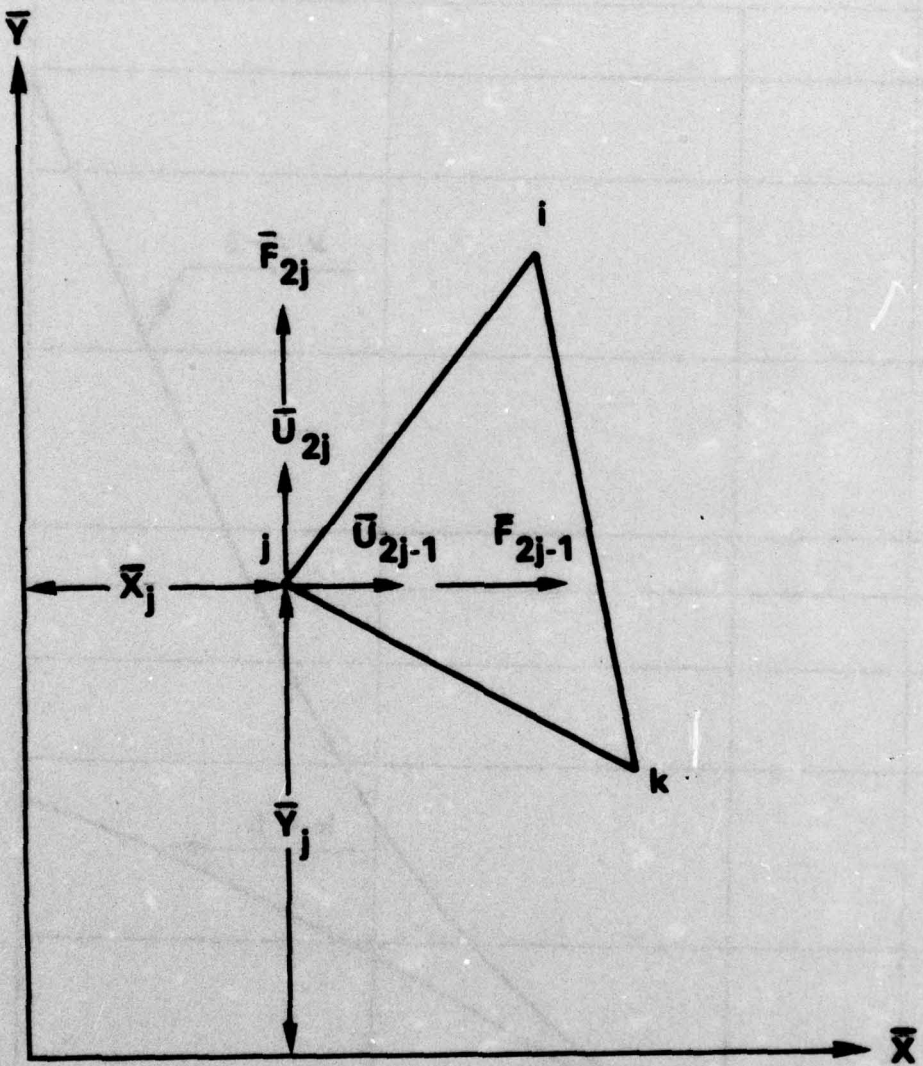


FIG. 7 COORDINATES, DISPLACEMENTS, AND FORCES OF THE j -th NODAL POINT

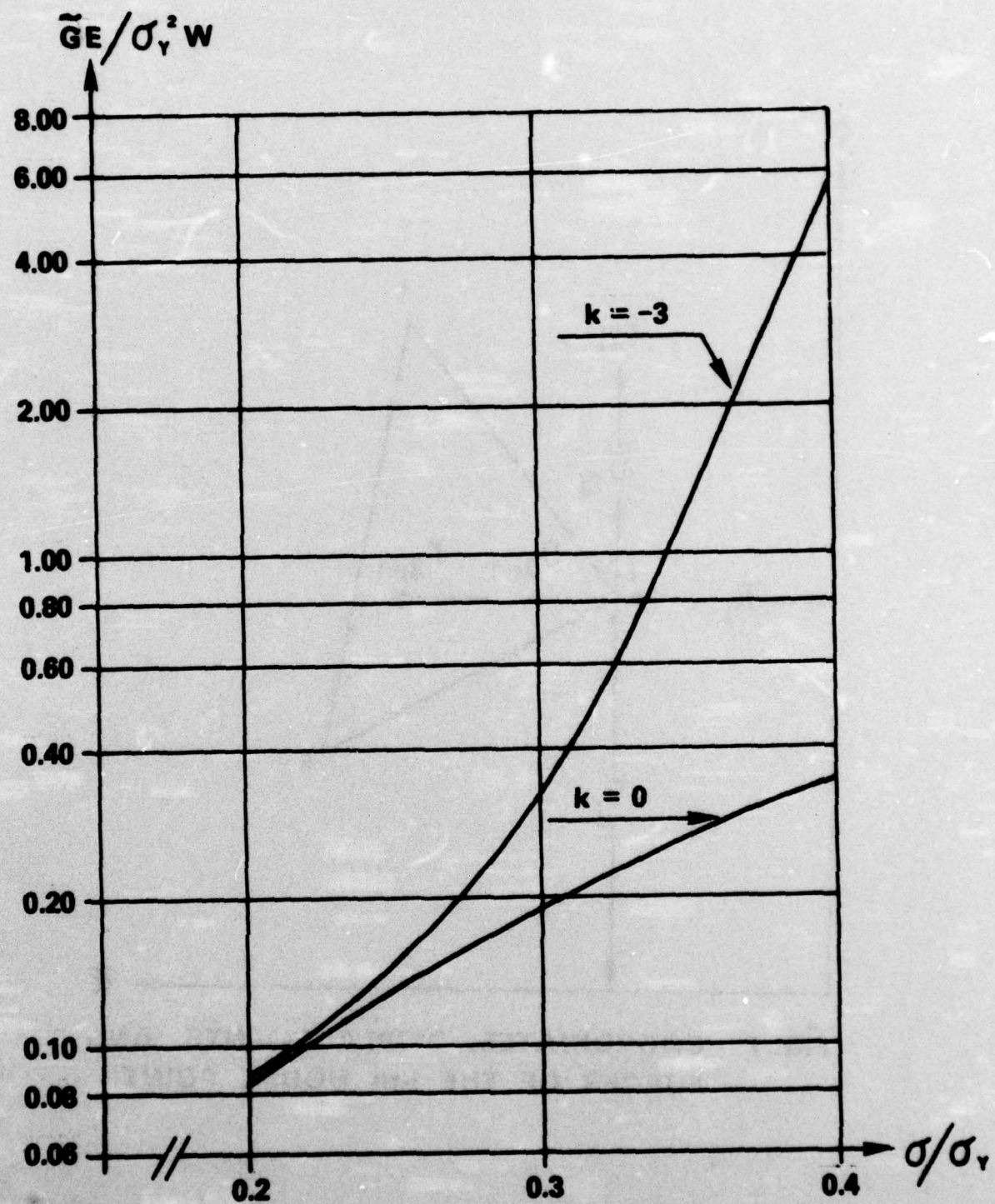


Fig. 8 Energy Release Rate vs Applied Stress
 $\nu = 0.33, \bar{\alpha} = 0.02, n = 13, \ell = 2.5, c = 0.5$

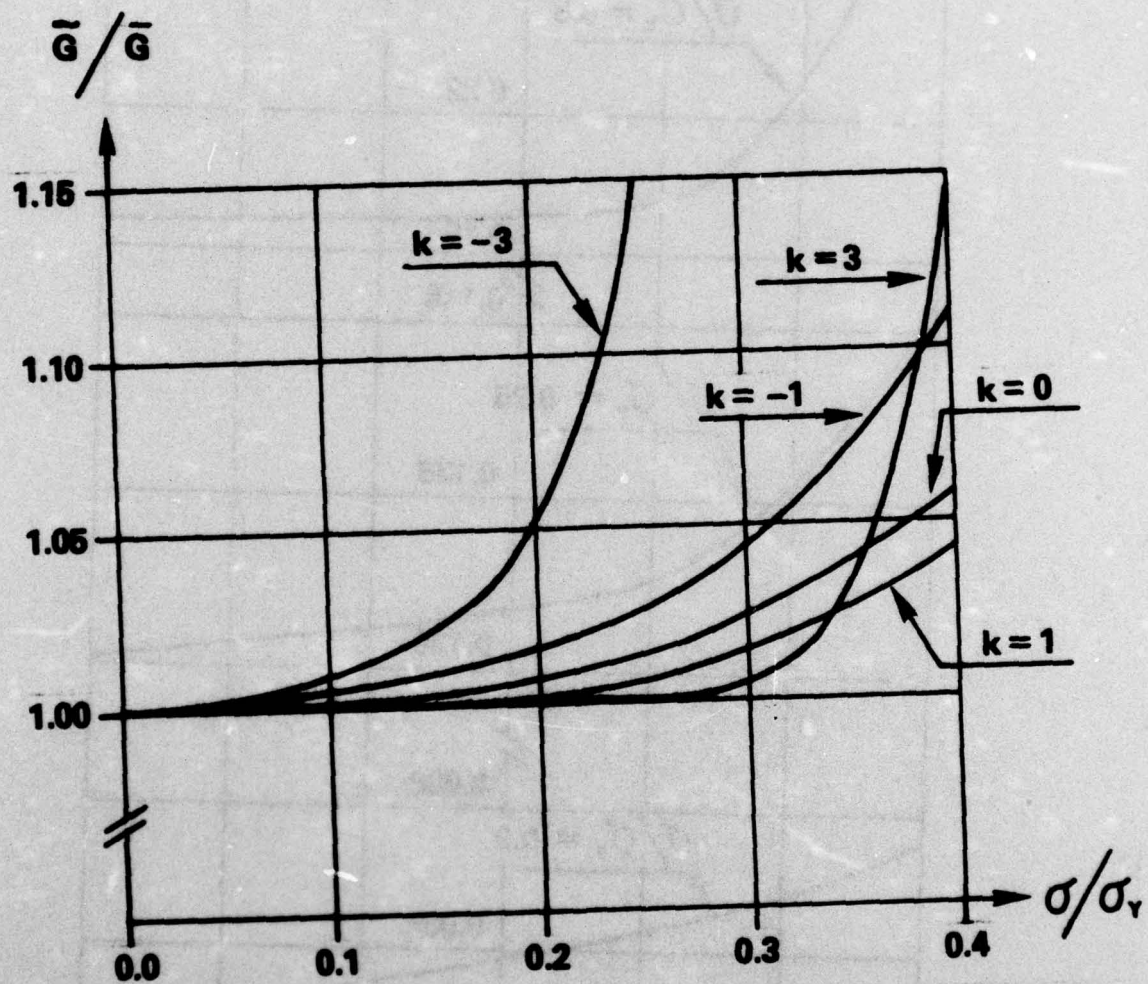


Fig. 9 Biaxial and Nonlinear Effects on Energy Release Rate
 $\nu = 0.33, \bar{\alpha} = 0.02, n = 13, \lambda = 13, c = 0.5$

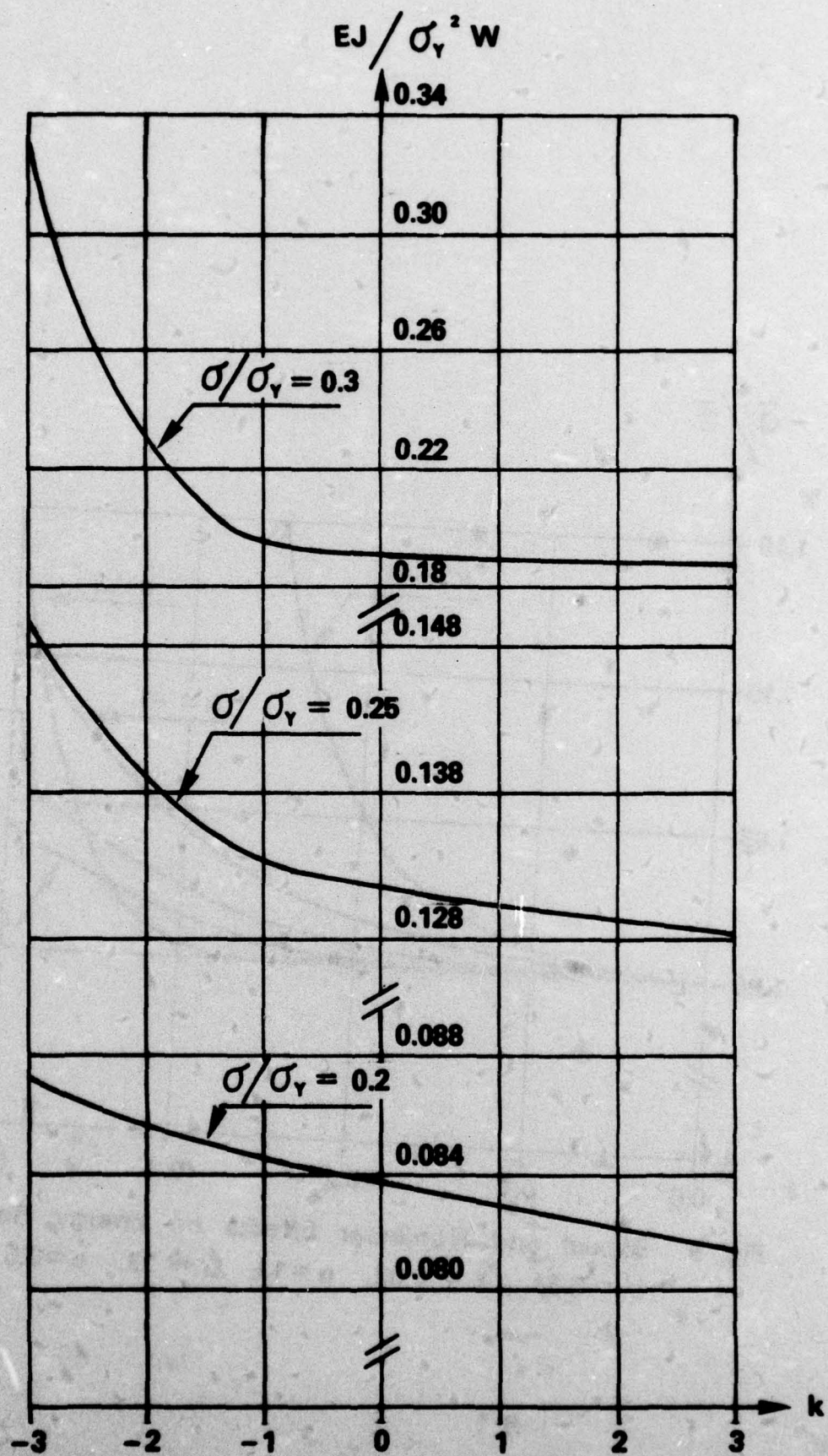
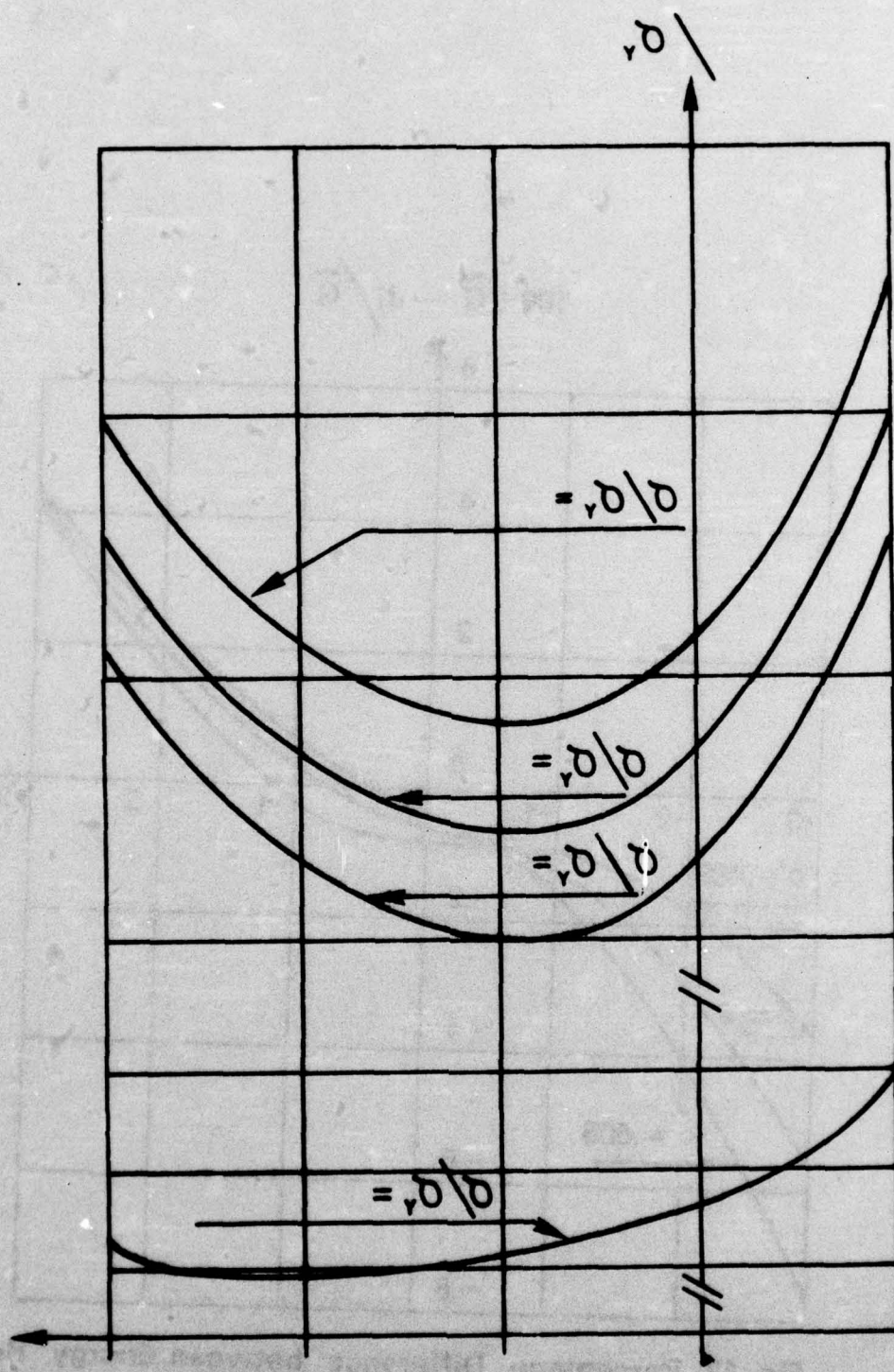


Fig. 10 J-integral vs Biaxial Load Factor

$$V = 0.33, \bar{\alpha} = 0.02, n = 13, \ell = 2.5, c = 0.5$$



$-\lambda$ $-\delta$ $-v$

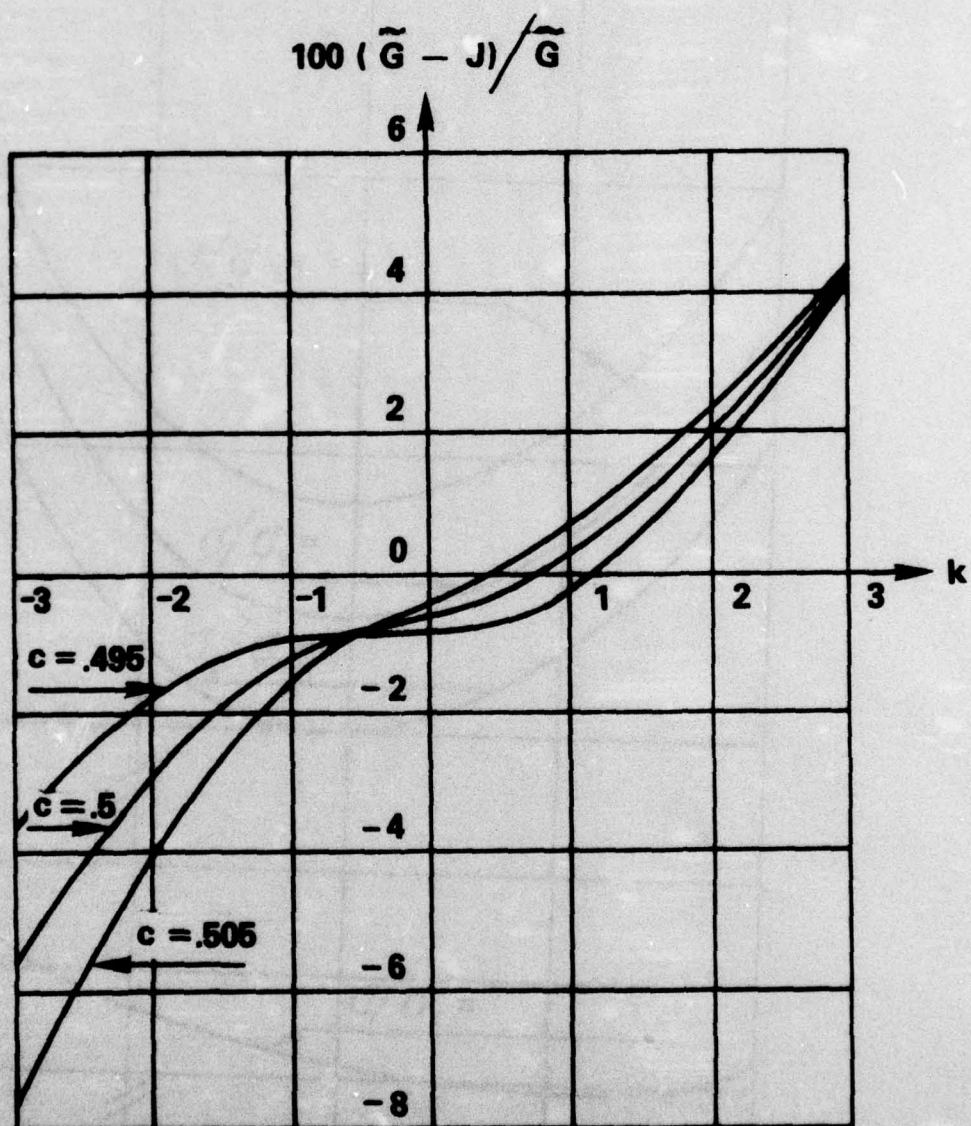


Fig. 12 Percentage Difference between Energy Release Rate and J-integral

$\nu = 0.33, \bar{\alpha} = 0.02, n = 13, \lambda = 2.5, \sigma / \sigma_y = 0.4$

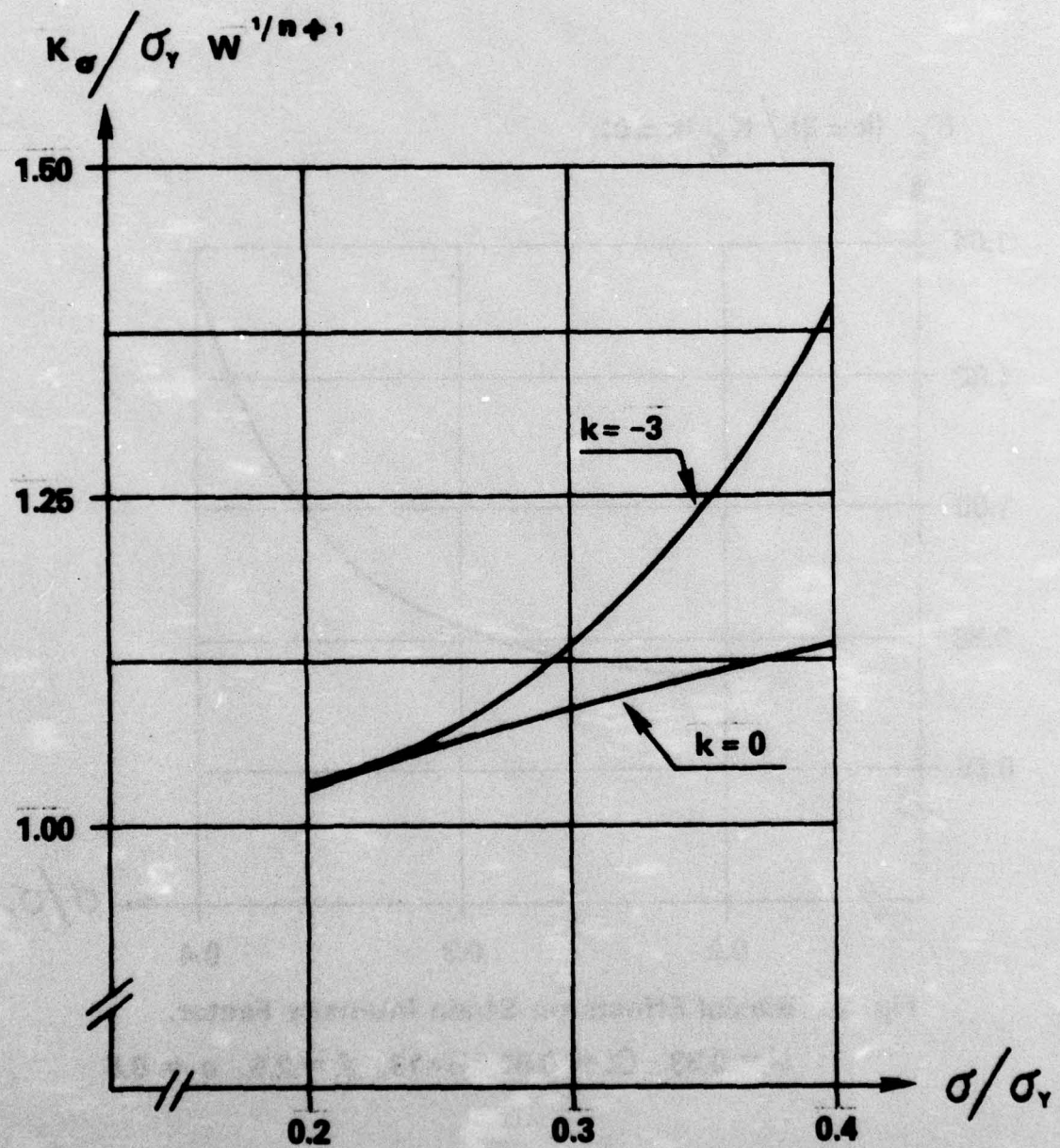


Fig. 13 Stress Intensity Factor vs Applied Stress

$$\nu = 0.33, \bar{\alpha} = 0.02, n = 13, l = 2.5, c = 0.5$$

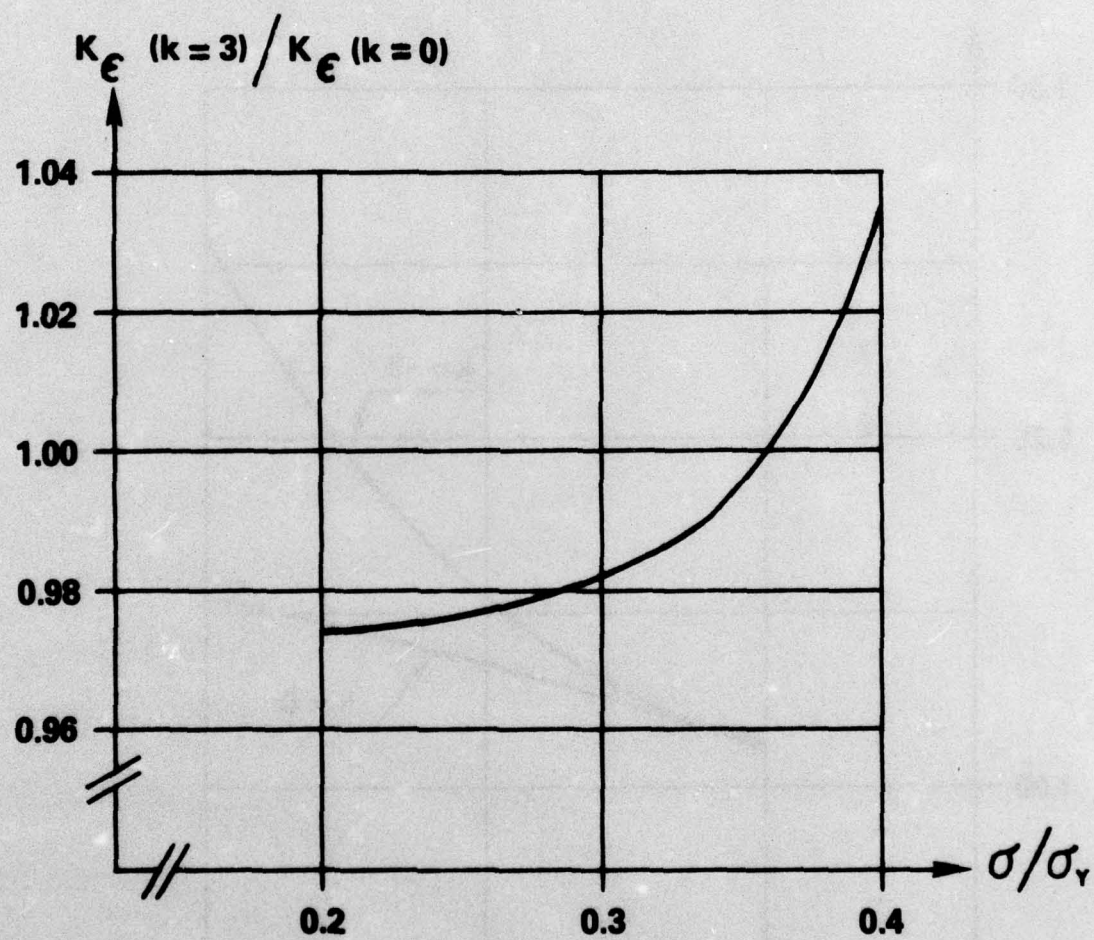


Fig. 14 Biaxial Effects on Strain Intensity Factor,

$$\nu = 0.33, \bar{\alpha} = 0.02, n = 13, \lambda = 2.5, c = 0.5$$

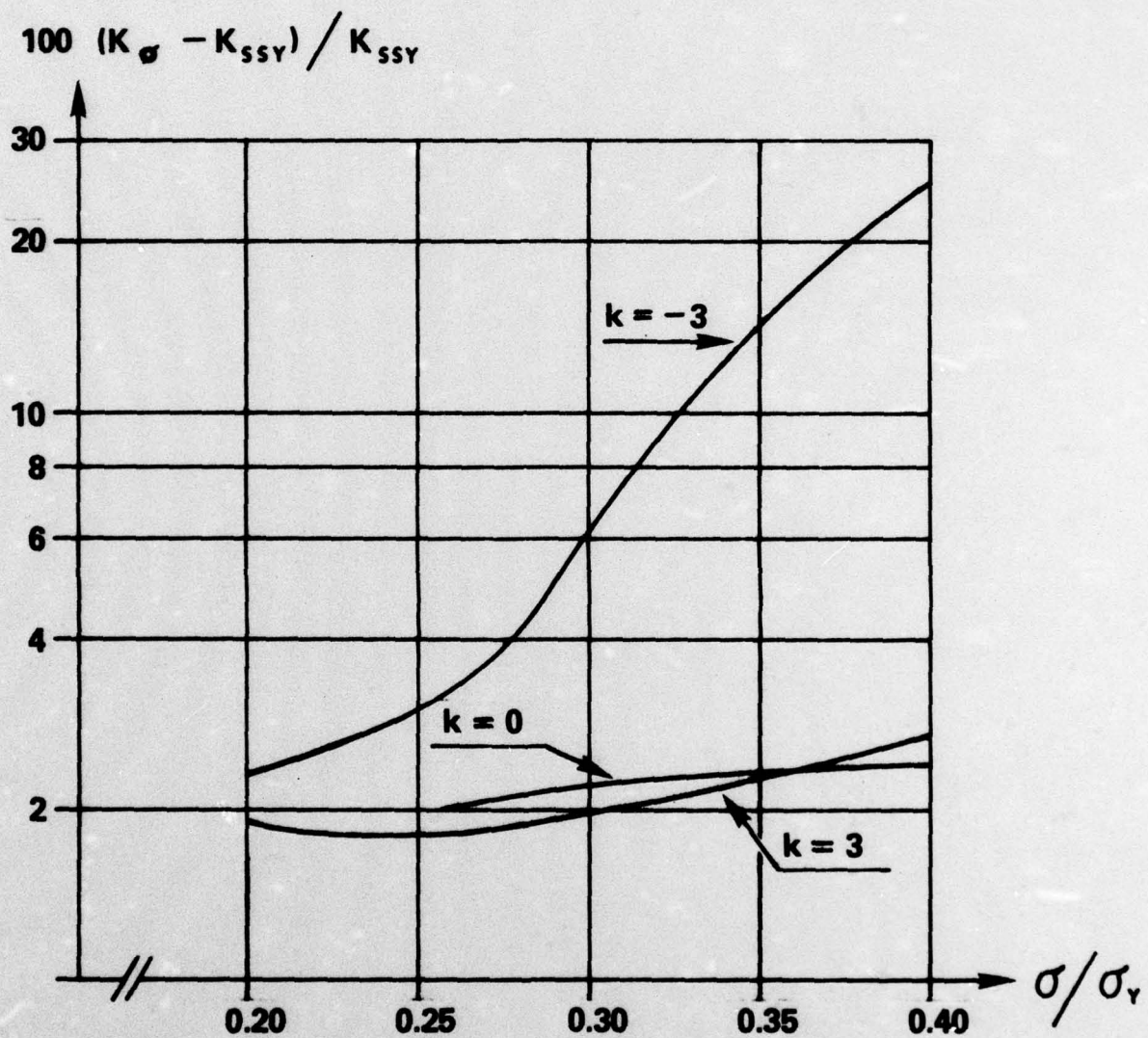


Fig. 15 Biaxial and Nonlinear Effects on Stress Intensity Factor
 $\nu = 0.33, \bar{\alpha} = 0.02, n = 13, l = 2.5, c = 0.5$

DD FORM 1 JAN 73 1473 EDITION OF 1 NOV 65 IS OBSOLETE
S/N 0102-014-6601

UNCLASSIFIED

SECURITY CLASSIFICATION OF THIS PAGE (When Data Entered)

20 ABSTRACT (continue)

→ crack. Biaxial effects on fracture toughness parameters increase as applied stress increases. The coupling between biaxial effects and material nonlinearity has been indicated.

THE GEORGE WASHINGTON UNIVERSITY

BENEATH THIS PLAQUE
IS BURIED
A VAULT FOR THE FUTURE
IN THE YEAR 2056

THE STORY OF ENGINEERING IN THIS YEAR OF THE PLACING OF THE VAULT AND
ENGINEERING HOPES FOR THE TOMORROWS AS WRITTEN IN THE RECORDS OF THE
FOLLOWING GOVERNMENTAL AND PROFESSIONAL ENGINEERING ORGANIZATIONS AND
THOSE OF THIS GEORGE WASHINGTON UNIVERSITY.

BOARD OF COMMISSIONERS DISTRICT OF COLUMBIA
UNITED STATES ATOMIC ENERGY COMMISSION
DEPARTMENT OF THE ARMY UNITED STATES OF AMERICA
DEPARTMENT OF THE NAVY UNITED STATES OF AMERICA
DEPARTMENT OF THE AIR FORCE UNITED STATES OF AMERICA
NATIONAL ADVISORY COMMITTEE FOR AERONAUTICS
NATIONAL BUREAU OF STANDARDS U.S. DEPARTMENT OF COMMERCE
AMERICAN SOCIETY OF CIVIL ENGINEERS
AMERICAN INSTITUTE OF ELECTRICAL ENGINEERS
THE AMERICAN SOCIETY OF MECHANICAL ENGINEERS
THE SOCIETY OF AMERICAN MILITARY ENGINEERS
AMERICAN INSTITUTE OF MINING & METALLURGICAL ENGINEERS
DISTRICT OF COLUMBIA SOCIETY OF PROFESSIONAL ENGINEERS, INC.
THE INSTITUTE OF RADIO ENGINEERS, INC.
THE CHEMICAL ENGINEERS CLUB OF WASHINGTON
WASHINGTON SOCIETY OF ENGINEERS
FALKNER, KINGSBURY & STEPHOUSE - ARCHITECTS
CHARLES H. TOMPKINS COMPANY - BUILDERS
SOCIETY OF WOMEN ENGINEERS
NATIONAL ACADEMY OF SCIENCES NATIONAL RESEARCH COUNCIL

THE PURPOSE OF THIS VAULT IS INSPIRED BY AND IS DEDICATED TO
CHARLES HOOK TOMPKINS, DOCTOR OF ENGINEERING

BECAUSE OF HIS ENGINEERING CONTRIBUTIONS TO THIS UNIVERSITY TO HIS
COMMUNITY TO HIS NATION AND TO OTHER NATIONS

BY THE GEORGE WASHINGTON UNIVERSITY

ROBERT V. FLEMING
CHAIRMAN OF THE BOARD OF TRUSTEES

CLOYD H. MARVIN
PRESIDENT

To cope with the expanding technology, our society must
be assured of a continuing supply of rigorously trained
and educated engineers. The School of Engineering and
Applied Science is completely committed to this ob-
jective.